Kathmandu University
Journal of Science, Engineering and Technology

Influence of tempering heat treatment on mechanical properties of welded mild steel

Surendra Sujakhu*[a], Balkrishna Chaudhary[a], Sabal Panthee[a], and Dadiram Dahal[b]

[a]Department of Mechanical Engineering, Kathmandu University, Dhulikhel, Kavre, Nepal.
[b]Turbine Testing Lab, Kathmandu University, Dhulikhel, Kavre, Nepal.

Abstract

An experimental study is performed in this research to investigate the changes in mechanical properties of mild steel during the welding and tempering heat treatment cycle. Four experimental cases were considered; i) as-received, ii) heat-treated, iii) welded, and iv) post-weld heat treated. Both the heat-treated and post-weld heat-treated cases followed the identical tempering process. Charpy and tensile tests were done to investigate the tested specimens' impact energy and fracture strength. A total of 16 tensile tests and 16 Charpy tests were conducted. Fracture surface studies were performed to determine the types of fracture on samples of all four cases. The results of the Charpy test according to the toughness of samples were: heat-treated > as-received > post-weld heat-treated > welded. Similarly, the tensile test results according to tensile strength were: heat-treated > as-received > post-weld heat-treated > welded. The hardness of samples was predicted from tensile strength, using the correlation of hardness and tensile strength of mild steel. The predicted hardness at four cases of samples was: heat-treated > as received > post-weld heat-treated > welded. It was observed that the strength of welded samples is less as compared to the as-received case and there was an increase in the strength of samples after being heat-treated and post-weld heat treated.

Keywords: Mild steel; Mechanical properties; Post Weld Heat Treatment (PWHT); Tempering

1. Introduction

The construction of different parts of the turbine requires different types of materials like stainless steel, carbon steel, High Strength Micro Alloy (HSMA), heat-treated steel, low carbon steel, etc. As mild steel displays good weldability and machinability, the parts of the turbine can be made of mild steel material. Most of the Nepalese hydropower runs in sediment-laden rivers where various types of degradations like oxidation effects, cavitation, crack formations, erosion, and wear are seen in turbine components during the regular operation of hydropower [1]. Maintenance of turbine components is done periodically for the efficient operation of hydropower. Material removal, welding, surface finishing, heat treatment, and other machining process are commonly used methods in the regular maintenance of turbines. The welding of different components of a turbine introduces defects like tensile residual stress, stress concentration, and other defects in the materials.

Many studies have been conducted to study the damage to hydraulic turbine components and their maintenance [1-5]. The case study of Kali Gandaki "A" (Fig. 1) done by Balendra Chhetry and Kumar Rana was focused on the effect of sand /silt abrasion and erosion on the turbine and its components. The repairing of turbine components was followed by welding, machining, HVOF coating, and heat-treating (for stress relieving) [1]. During the welding process, the weld metal is melted affecting adjacent base metal to create heat-affected zone (HAZ). Such local heating and cooling causes thermal expansion and contraction of the weld joint resulting into tensile residual stresses [2,6,7,8]. A study reported by Bayraktar et al. [4] investigated the mechanisms of grain growth in the welding joints of interstitial free steels. Examinations of the welded joints near the fusion line revealed the existence of significantly large grains aligned in the direction of heat flow. In the context of welding low-carbon steels, previous research [9,10] has emphasized the importance of the grain coarsened zone (GCZ) and heat-affected zone (HAZ) due to their susceptibility to embrittlement.

The tempering process of a welded joint involves heating the joint to a specific temperature and maintaining it at that temperature for a certain duration, followed by controlled cooling. This heat treatment process induces various mechanisms that contribute to the improvement of mechanical properties. The underlying mechanisms of the tempering process on a welded joint for the enhancement of mechanical properties studied previously has reported; reduction of residual stress [2,11], grain growth control [4], precipitation hardening [8], microstructural stability [6,7] and toughening [10] as the major reasons for the improvement in mechanical properties. The residual stress and other defects raised due to welding can be recovered by post-weld heat treatment (PWHT). Based on the study conducted on repair of Khimti Hydropower's Pelton turbine by Panthee et al. [5], it was reported that welding repair only did not exhibit satisfactory post repair operational lifespan. The study suggested that proper implementation of preheating, weld speed, and post-weld heat treatment is crucial to ensure successful repair of turbine. To remove residual tensile stress resulting from the welding process post-weld heat treatment is necessary, which also facilitates the diffusion of hydrogen present in the weld zone at higher temperatures, thereby reducing the risk of corrosion cracking and hydrogen-induced cracking. It is important to ensure an adequate soaking time during heat treatment and precise control of the cooling rate to achieve the desired mechanical properties at room temperature. The minimum required soaking time in PWHT was calculated using eq. 1.

*Corresponding author. Email: surendra.sujakhu@ku.edu.np

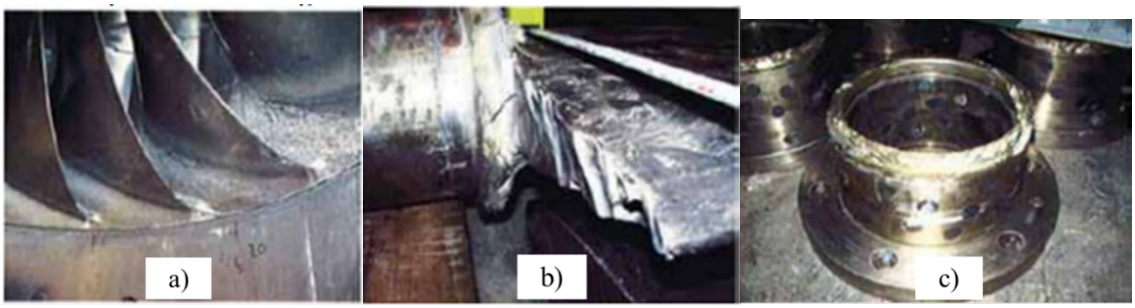

Figure 1: Damaged turbine components of unit 3, Kali Gandaki "A" Hydropower [1].

$$\text{Soaktime} = 0.2 \text{ hour/cm} \times \text{max. thickness in cm} + 2 \text{ hour} \quad (1)$$

The duration of the soaking period for heat treatment is influenced by factors such as the chemical composition of the material, thermal history of the component, initial microstructure, Maximum size and weight of the section. In cases where the part has varying cross-sections, the soaking period is determined by the largest cross-sectional area [11].

Olabi and Hashmi [12] had conducted detailed study on PWHT for low carbon steel. The study had considered different PWHT parameters such as soaking time, temperature and cooling rate. The heating rates of PWHT were 400°C/hr, 100°C/hr and 50°C/hr, soaking temperatures were 450°C, 550°C and 650°C, holding times were 2hr, 0.5hr and 10hr, and cooling rates were 40°C/hr, 10°C/hr and 125°C/hr. For the removal of residual stresses in welded component, the PWHT temperature of 650 °C was found to be effective. It was observed that there is no significant effect on the heating rate as compared to holding time, holding temperature, and cooling rate. Prolonged heating time with slower cooling rates were reported to exhibit better properties and result after PWHT process [12]. The range of notch toughness at different tempering temperatures is illustrated in Fig. 2. The notch toughness gradually increases with higher tempering temperatures and a higher value for lower carbon content.

In the context of Nepal, Mild steel has wide use in micro-hydropower and other fields and technology. The effect of welding process and heat treatment process has been studied in mild steel for other applications [13,14]. The experimental study aims to investigate the changes in the strength of mild steel when subjected to the welding and heat-treatment process. There are different types of heat treatment processes like annealing, normalizing, case hardening, hardening, tempering, etc. Among those processes, tempering is done. More concern is given to post-weld heat treatment of mild steel as different turbine components maintenance includes welding and heat treatment processes in Nepalese hydropower. The strength of mild steel can be determined by different destructive tests like a tensile test, Charpy test, hardness test, fatigue test, etc. Different parameters of mechanical properties of mild steel can be obtained from those destructive tests. Fractography study and examination of the fractured surface and its characteristics can aid in identification of the underlying causes of material failure. Different failure modes result in distinct characteristics on the fracture surface which supports to identify the root cause of the failure. For engineering materials, generally, two types of mechanisms are seen in materials: ductile fracture and brittle fracture. Ductile fracture involves huge plastic deformation and brittle fracture exhibits the failure of material without or with very less plastic deformation [15,16]. The crack in brittle fractures spread rapidly and catastrophically without any warning once initiated. Brittle fracture is characterized by very less to no plastic

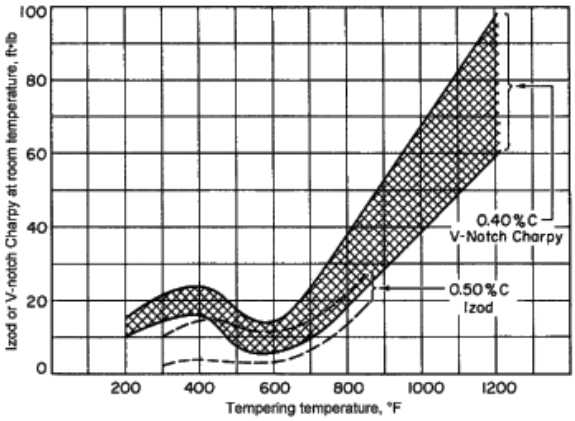

Figure 2: Range of notch toughness at room temperature after various tempering temperatures [0.40 and 0.50% C] [17].

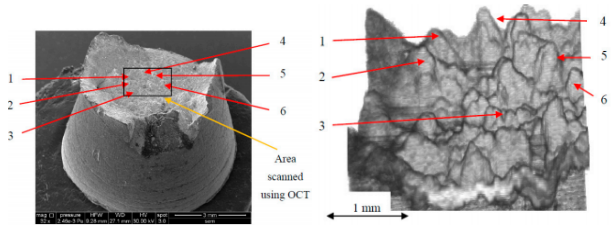

Figure 3: Frontal SEM overview of the entire sample for OCT investigation (left), OCT image obtained with MS/SS-OCT system (right) [18].

deformation and failure occurs below the yield strength of the material. Brittle fracture can normally be identified by the smoothness of the fractured surface.

An experimental investigation was conducted by Hutiu et al. [18] involving variety of metals, including low carbon steels, stainless steels, graphite cast irons, high-quality rolled steel and antifriction alloy. Optical Coherence Tomography (OCT) and Scanning Electron Microscopy (SEM) analysis were performed on the tensile tested specimen to assess the occurrence of ductile and brittle fractures in the studied metals as shown in Fig. 3. The SEM analysis served as a means of validating the findings obtained from the OCT images. The results revealed that the fracture surfaces of the low carbon samples exhibited cup and cone features, which were indicative of the ductile mode of fracture.

2. Materials and methods

2.1. Materials

The chemical composition of the ASTM A36 mild steel sample used in this study is presented in Table 1 below. Mild steel has a relatively high melting point of between 1450°C to 1520°C. The

Table 1: Chemical composition of ASTM A36 Mild steel.

Elements	Wt.%
Mn	0.1
Si	0.28
P	0.04
S	0.1
C	0.29
Fe	98.14
Cu	0.2

Table 2: Four cases of experiment.

Case 1	Destructive test of the originally received sample
Case 2	Destructive test of the welded sample
Case 3	Destructive test of the tempered original sample
Case 4	Destructive test of the welded sample after post-weld heat treatment

elevated melting temperature of mild steel results in increased ductility when heated, making it well-suited for forging, cutting, drilling, and easy fabrication through welding. A general-purpose mild steel block used and available for structural application was used in this work to manufacture test specimens for investigating mechanical properties.

2.2. Experimental design

The investigation of changes in the strength of welded and post-weld heat-treated mild steel samples was followed by four cases. The four cases considered to investigate the changes in the strength of mild steel samples are listed in Table 2. The destructive test done to determine the strength of mild steel samples in different cases are the tensile and Charpy tests. Each case uses 8 samples for the experiment [4-Tensile test, 4-Charpy test]. The total number of samples used for the experiment is 32.

The whole experiment was carried out based on the facilities available at Kathmandu University. A muffle furnace with a PID controller of the FY400 series has been used for heating purposes. A fracture study was done to determine the type of fracture of samples. The fracture surface of every sample was examined using a Stereo zoom microscope of the RSM-9 series model. UTM machine (Model: UTN 10, serial No.:5/90-1307) has been used for the tensile test. A Charpy test machine of capacity 300J has been used for the Charpy test and the Hardness of the material is predicted using the tensile strength of samples. E.J Pavlina and C.J Van Tyne [19] reported existence of correlation between yield strength, tensile strength and hardness for steel. A linear relationship was reported between the yield strength, tensile strength, and hardness for steels with yield strengths ranging from 325 MPa to 1700 MPa, and tensile strengths ranging from 450 to 2350 MPa. The prediction of hardness has been done using a correlation between tensile strength and the hardness of the material. The least-squares linear regression (eq. 2) gives the correlation for tensile strength [20].

$$TS = C_3 \times RH^3 + C_2 \times RH^2 + C_1 \times RH + C_0 \qquad (2)$$

Where, TS: Tensile strength; RH: Rockwell Hardness; C_3, C_2, C_1 and C_0 are the coefficient whose value for scale B (for mild steel) are: 0.0006, -0.1216, 9.3502 and -191.89 respectively.

Although the obtained values of hardness do not reflect the exact value of hardness of mild steel, it provides linear changes in values of hardness concerning tensile strength.

2.3. Experimental specimens

Sample machining was done to attain a standard size of the sample for the destructive test. The mild steel rod was machined into the shape of a tensile test specimen and Charpy test specimen in consideration to the ASTM standard E8 for tensile and ASTM standard E23 for Charpy test. The designed samples with dimensions are given in Fig. 4.

For the welded specimens, the original mild steel samples as shown in Fig. 4 were cut and groves were created as shown in Fig. 5 which were then filled by using arc welding, finally, the welded filled specimens were machined to their standard size. The Charpy test samples were cut in a V-shaped middle with a 10mm length of cut at the upper surface and 2 mm clearance at the lower part of the sample (Fig. 5a)). The tensile test samples were cut 10 mm against the middle of the gauge part (Fig. 5b)). Shielded metal arc welding (SMAW) with E60 electrode process was used to fill those welding grooves in the test samples. Manual two pass welding was performed to completely fill the grooves. The welded samples were surface-finished and brought back to the orientation for the destructive test. To determine the mechanical properties of weld filled part (weld material) along with weld joints in both heat-treated and untreated cases, weld filling was done on the sample, instead of only weld joining in this experiment.

Sample cut for weld filling (All dimensions are in mm.)

2.4. Tempering heat treatment process

The heat treatment cycle used for tempering in this study is presented in Fig. 6. The tempering heat treatment cycle is for both initially machined samples (case 3) as well as welded samples (case 4). The tempering temperature of 450°C was considered based on Fig. 2, to obtain approximately maximum toughness and stress relief with minimum loss in other strengths. The total time of the heat treatment cycle was considered based on working hours a day. The PID program was set based on the heating rate and holding time mentioned in Fig. 6. Holding time was calculated using eq. 1. The samples were left in the furnace to cool naturally inside it. On observing the time and temperature of cooling the samples, the samples were cooled approximately at a cooling rate of 20°C/hr.

2.5. Study of fracture surface

No preprocessing was required for the fractography study of fractured samples. The fracture surface was examined using Stereo-Zoom microscope with magnification from 7X to 45X. The samples were placed one by one on the stage plate. The top light was provided on the fracture surface of the sample. The position, magnification, and focus knob were adjusted to observe the fracture surface. The inspection was done on fractured samples after the destructive test with different magnifications (14X to 45X). Photographs of fractured parts and fracture surfaces for the record were taken using a mobile camera.

2.6. Computation of variations in the results

The destructive test done on samples showed some variation in results between each sample, although the procedure and material are the same. Standard deviation was calculated to measure the extent of results variation and account for all forms of random error, such as machine variability, material variability, and the anticipated variations inherent in adhering to the standard test procedure. Computation of mean and standard deviation has been done using eq. 3 and 4 [21].

$$\overline{y} = \frac{\sum_{i=1}^{n} y_i}{n} \qquad (3)$$

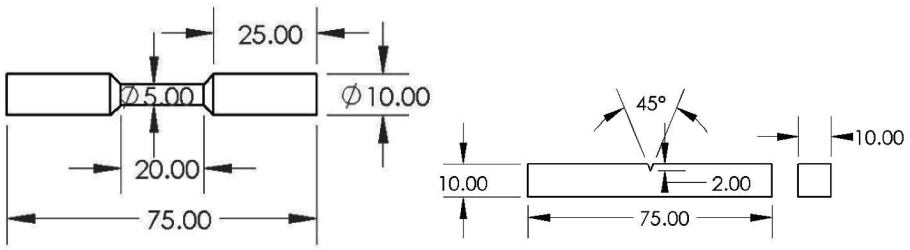

(a) Tensile test sample (b) Charpy test sample.

Figure 4: Designed samples. All dimensions are in mm.

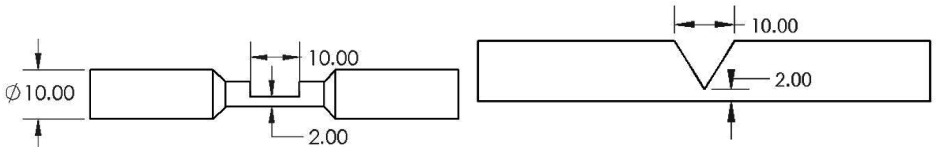

(a) Tensile test sample (b) Charpy test sample.

Figure 5: Sample cut for weld filling. All dimensions are in mm.

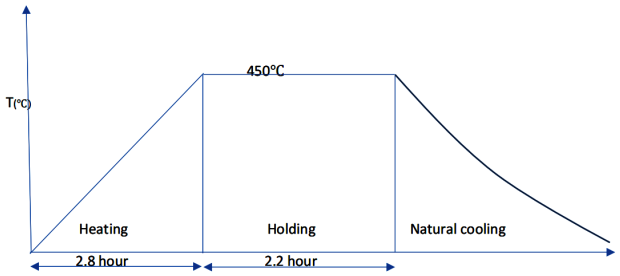

Figure 6: Tempering heat treatment cycle.

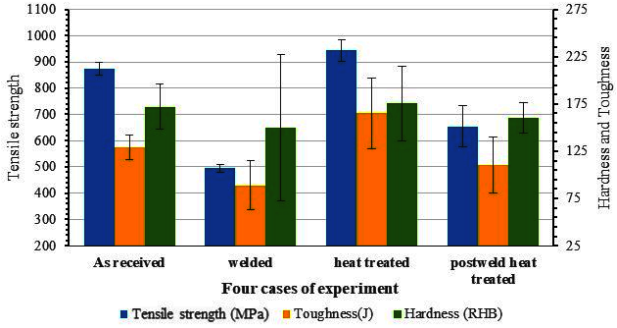

Figure 7: Column chart Mechanical properties of mild steel in four cases.

Table 3: Mechanical properties of test specimens.

Cases	Toughness (J)	Tensile strength (MPa)	Hardness (RHB)
As received	129	875.18	172.153
Welded	89	494.75	149.633
Heat-treated	165	943.28	175.33
Post weld heat treated	110.5	654.67	160.355

$$s = \sqrt{\frac{\sum_{i=1}^{n} (y_i - \overline{y})^2}{n-1}} \tag{4}$$

3. Results and discussion

3.1. Destructive testing result

The measurement results of the destructive test in different cases are presented in Table 3 and plotted in Fig. 7.

The data extracted from the tensile test are not the accurate value of mechanical properties, as the UTM machine was not in good condition to provide the exact result of tensile strength. The breaking strength observed in the test is considered tensile strength. However, the data extracted using the available UTM machine can provide a comparative study to determine the effect of all four cases on the mechanical properties of the mild steel sample. The hardness is calculated based on the correlation between tensile strength and hardness in eq. 2.

The welded mild steel samples exhibit low toughness, tensile strength, and hardness as compared to other cases samples. However, those mechanical properties are improved in post-weld heat-treated samples than in welded samples. The heat-treated samples show high strength as compared to other cases. The tempering process increased the strength of the mild steel sample. Fig. 7 shows the graphical representation of the comparison of mechanical properties of mild steel samples in four cases. The error bar in each column is based on the standard deviation calculated using eq. 4. The variation and range of results are determined using standard deviation. As received samples do not show more variations in results, as compared to samples of other cases. Although the samples were subjected to a particular tempering process, different machining and surface finishing process was done on the samples. This machining process affects the strength of the material. The dimension of the samples was not precisely identical, especially the notch of the Charpy test sample. The exact dimension of the prepared samples was not ensured with the designed dimension. Some tolerance was seen in the sample dimension, as it was prepared manually. Also, the improper and un-identical welding on welded samples resulted in variations in the resultant strength of the samples.

3.2. Fracture study

Microscopic examination was carried out on the fracture surface of samples after the destructive test (Fig. 8). The fracture surface of each sample was examined to determine the type of fracture in mild steel. Fig. 9 and Fig. 10 show the fracture surface of the mild steel sample after Charpy and tensile tests respectively in all four cases.

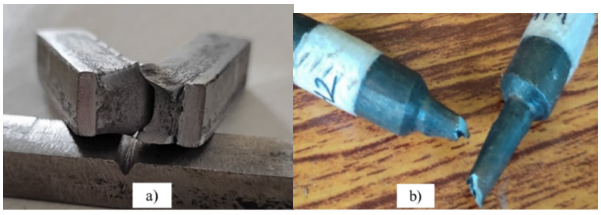

Figure 8: Image of samples after the destructive test. (a) Charpy test sample (b) Tensile test sample.

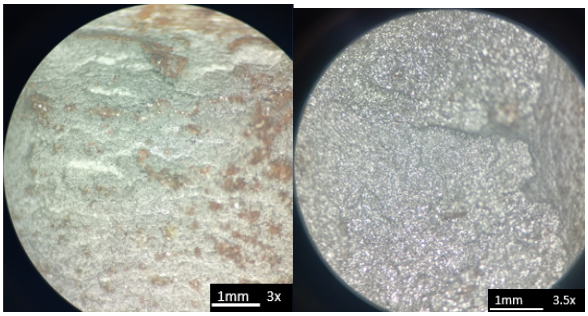

(a) Original. (b) Welded.

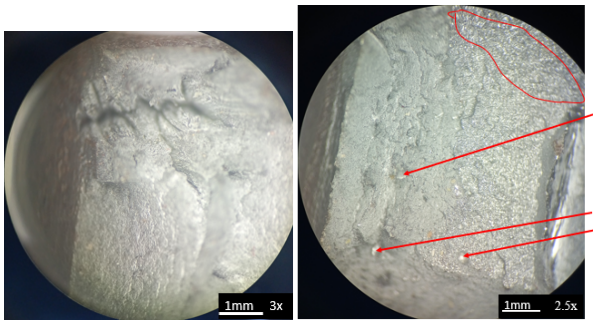

(c) Heat-treated. (d) Welded and heat-treated.

Figure 9: Images of fracture surface after Charpy test.

In general, study of all the fracture surface showed relatively ductile nature of fracture. However, slight difference in the fracture study was observed for different cases of the specimens. Fig. 9 presents the fracture surface of the Charpy tested specimens. Mostly transgranular nature of fracture could was observed in the impact tested specimen illustrative of ductile nature of the fracture process. In case of the welded specimen fracture surface (Fig. 9b), slightly brittle fracture surface was observed indicative of the effect of the welding process. In case of heat treated specimens, ductile fracture surface with some evident of microvoids formation (Fig. 9d) was observed.

The fracture surfaces of the tensile tested specimens are presented in Fig. 10. Some dimple ruptures along with the uneven surface pattern were seen on the surface of the original sample. It notifies that the fracture is ductile in originally prepared samples of mild steel. The welded samples have smooth and shiny fracture surfaces; this property shows the characteristics of brittleness or a decrease in ductility of the material. This shiny surface is only seen in welded parts of mild steel. However, the tensile sample in Fig. 10b is broken with some elongation in length and reduction in the cross-section area. It displays ductile fracture of mild steel even after weld filling with decreasing ductility of the sample. However, the tensile sample in Fig. 10b is broken with some elongation in length and reduction in the cross-section area. It displays ductile fracture of mild steel even after weld filling with decreasing ductility of the sample. The heat-treated sample has a more uneven fracture surface than that of the original sample. The irregular

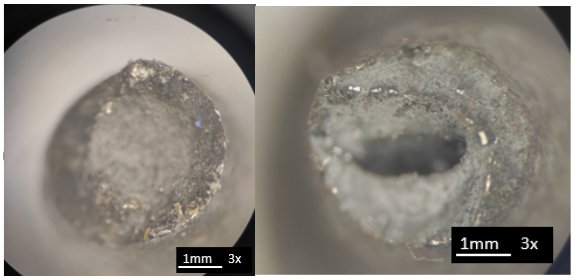

(a) Original. (b) Welded.

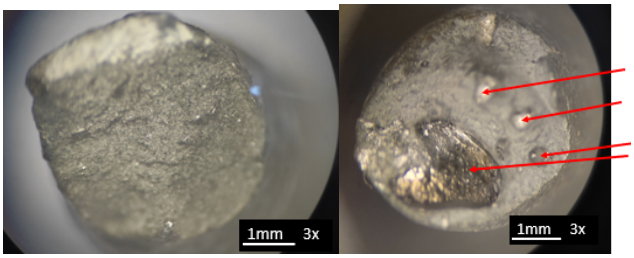

(c) Heat-treated. (d) Welded and heat-treated.

Figure 10: Images of fracture surface after tensile test.

surface formed at the fracture surface exhibits the ductile nature of the fracture. So, heat-treated samples seem to be more ductile than the original ones. Although the tensile test sample of all cases shows the cup and cone profile of fracture. But the appearance of the fibrous structure and bigger dimple rupture is seen more in the heated sample.

4. Conclusions

The order of samples according to their resultant toughness is heat-treated (165J) > as received (129J) > post-weld heat-treated (110J) > welded (89J). It is seen that; the toughness increases when mild steel is tempered. The order of sample based on their resultant tensile strength is heat-treated (943.28 MPa) > as-received (876.18 MPa) > post-weld heat-treated (654.67 MPa) > welded (494.75 MPa). Similarly, the hardness of samples is predicted from tensile strength, using the correlation between hardness and tensile strength of mild steel. Welded and post-weld heat-treated samples show lower values for tensile strength. It happened as a result of the specimen's faulty weld filling, which caused porosity to appear on the welded samples. Tensile test result indicated increased in tensile strength along with the improvement in elongation for the heat treated sample as compared to the welded sample. Such improvement in properties is mainly due to graphitization of the precipitated carbides which favors the formation of ferrite at the tempering temperature of 450°C.

The strength of mild steel gets reduced when subjected to welding and other machining processes during the repair and maintenance of turbine components. The heat treatment after the maintenance somehow increases the strength of turbine components. The samples that were subjected to tempering in this experiment exhibits superior mechanical properties as compared to other cases in term of toughness, hardness, and tensile strength. It concludes that maintenance of the turbine by welding process should be followed by a tempering heat treatment process to reduce heat-affected zones and possible accumulation of residual stresses. In addition, preheating steps should be applied under certain circumstances to prevent hydrogen-induced cracking after the welding. The diffusion of hydrogen after welding increases during the increased temperature of turbine components. It prevents excessive loss in ductility of mild steel turbines in the welded and heat-affected zone.

References

[1] Chhetry B & Rana K, Effect of sand erosion on turbine components: A case study of kali gandaki "a" hydroelectric project (144 mw), nepal, *Hydro Nepal: Journal of Water, Energy and Environment*, 17 (2015) 24–33.

[2] Silva C C, de Assis J T, Philippov S & Farias J P, Residual stress, microstructure and hardness of thin-walled low-carbon steel pipes welded manually, *Materials Research-ibero-american Journal of Materials*, 19 (2016) 1215–1225.

[3] Kattel S, Bhatt J P, Subedi R, Thapa B, Sujakhu S, Kafle A & Shakya T M, Investigation of mechanical properties of brass francis turbine manufactured by local investment casting technique in nepal, *Journal of Physics: Conference Series*, 1608(1) (2020) 012013. doi:10.1088/1742-6596/1608/1/012013. URL https://dx.doi.org/10.1088/1742-6596/1608/1/012013.

[4] Bayraktar E, Kaplan D, Devillers L & Chevalier J, Grain growth mechanism during the welding of interstitial free (if) steels, *Journal of Materials Processing Technology*, 189(1) (2007) 114–125. ISSN 0924-0136. doi:https://doi.org/10.1016/j.jmatprotec.2007.01.012. URL https://www.sciencedirect.com/science/article/pii/S0924013607000325.

[5] Panthee A, Thapa B & Neopane H P, Quality control in welding repair of pelton runner, *Renewable Energy*, 79 (2015) 96–102. ISSN 0960-1481. doi:https://doi.org/10.1016/j.renene.2014.10.042. URL https://www.sciencedirect.com/science/article/pii/S0960148114006697, selected Papers on Renewable Energy: AFORE 2013.

[6] Hafez K M, Ramadan M, Fathy N & Ismail M, Microstructure and mechanical properties of laser welded dual phase and mild steel joints for automotive applications, *Applied Mechanics and Materials*, 865 (2017) 81–87. doi:10.4028/www.scientific.net/amm.865.81.

[7] Pandey C, Mahapatra M, Kumar P, Kumar S & Sirohi S, Effect of post weld heat treatments on microstructure evolution and type IV cracking behavior of the p91 steel welds joint, *Journal of Materials Processing Technology*, 266 (2019) 140–154. doi:10.1016/j.jmatprotec.2018.10.024.

[8] Pandey C, Mahapatra M M, Kumar P, Thakre J & Saini N, Role of evolving microstructure on the mechanical behaviour of p92 steel welded joint in as-welded and post weld heat treated state, *Journal of Materials Processing Technology*, 263 (2019) 241–255. doi:10.1016/j.jmatprotec.2018.08.032.

[9] Firrao D, Matteis P, Spena P R & Gerosa R, Influence of the microstructure on fatigue and fracture toughness properties of large heat-treated mold steels, *Materials Science and Engineering: A*, 559 (2013) 371–383. doi:10.1016/j.msea.2012.08.113.

[10] Silwal B, Li L, Deceuster A & Griffiths B, Effect of postweld heat treatment on the toughness of heat-affected zone for grade 91 steel, *Weld. J*, 92(92) (2013) 80s–87s.

[11] Banerjee M. 2.1 fundamentals of heat treating metals and alloys. In: *Comprehensive Materials Finishing*. Elsevier (2017), pp. 1–49. doi:10.1016/b978-0-12-803581-8.09185-2.

[12] Olabi A & Hashmi M, Stress relief procedures for low carbon steel (1020) welded components, *Journal of Materials Processing Technology*, 56(1) (1996) 552–562. ISSN 0924-0136. doi:https://doi.org/10.1016/0924-0136(95)01869-7. URL https://www.sciencedirect.com/science/article/pii/0924013695018697, international Conference on Advances in Material and Processing Technologies.

[13] Sultana M N, Hasam M F & Islam M. Analysis of mechanical properties of mild steel applying various heat treatment (2014).

[14] Zhang C, Li G, Gao M & Zeng X, Microstructure and mechanical properties of narrow gap laser-arc hybrid welded 40 mm thick mild steel, *Materials*, 10(2) (2017) 106. doi:10.3390/ma10020106.

[15] Aloraier A, Ibrahim R & Ghojel J, Eliminating post-weld heat treatment in repair welding by temper bead technique: role bead sequence in metallurgical changes, *Journal of Materials Processing Technology*, 153-154 (2004) 392–400. doi:10.1016/j.jmatprotec.2004.04.383.

[16] Javidan F, Heidarpour A, Zhao X L, Hutchinson C R & Minkkinen J, Effect of weld on the mechanical properties of high strength and ultra-high strength steel tubes in fabricated hybrid sections, *Engineering Structures*, 118 (2016) 16–27. doi:10.1016/j.engstruct.2016.03.046.

[17] Dossett J L & Totten G E, eds. *Steel Heat Treating Fundamentals and Processes*. ASM International (2013). doi:10.31399/asm.hb.v04a.9781627081658.

[18] Hutiu G, Duma V F, Demian D, Bradu A & Podoleanu A G, Assessment of ductile, brittle, and fatigue fractures of metals using optical coherence tomography, *Metals*, 8(2). ISSN 2075-4701. doi:10.3390/met8020117. URL https://www.mdpi.com/2075-4701/8/2/117.

[19] Pavlina E & Tyne C V, Correlation of yield strength and tensile strength with hardness for steels, *Journal of Materials Engineering and Performance*, 17(6) (2008) 888–893. doi:10.1007/s11665-008-9225-5.

[20] Lancaster S. Sciencing: How to convert rockwell hardness to tensile strength. Online (2018). URL https://sciencing.com/convert-rockwell-hardness-tensile-strength-8759475.html.

[21] Splett J, Iyer H, Wang C M J & McCowan C. Computing uncertainty for charpy impact machine test results (2008). doi:10.13140/RG.2.1.4476.9683.